

and evaporated to give an oil. The oil was crystallized from chloroform–light petroleum (b.p. 40°–60°C) to give 4-acryloyl-1-methyl-2,6-piperazinedione (3; R = Me) (3.34 g, 89%) as a white crystalline solid m.p. 75°–77°C.  $C_8H_{10}N_2O_3$  Calculated: C 52.79 H 5.54 N 15.39;  $M$ , 182. Found: C 52.63 H 5.53 N 15.30  $M^+$  182,  $^1H$  n.m.r. [ $(CD_3)_2CO$ ]:  $\delta$  = 6.6–7.1 (m, 1H, HC=), 5.6–6.35 (m, 2H,  $CH_2$ =), 4.55 (s, 4H,  $H_2C-N-CH_2$ ), 3.05 ppm (s, 3H, N- $CH_3$ ).

4-Acryloyl-1-hydroxy-2,6-piperazinedione (3; R = OH). 1-Hydroxy-2,6-piperazinedione was added to water (3  $cm^3$ ), the suspension was heated to 65°C and cooled to 0°C. Acryloyl chloride (0.35 g, 0.0039 mol) was added dropwise and the solution was stirred for 1 h. 4-Acryloyl-1-hydroxy-2,6-piperazinedione (3; R = OH) (1.13 g, 81%)

was deposited as a white solid m.p. 142° (from acetone-diethyl ether). Calculated:  $M$ , 184; Found:  $M^+$ , 184.

#### ACKNOWLEDGEMENTS

The Science Research Council and Koch-Light Laboratories Ltd are thanked for the provision of a CASE studentship (A.T.S.).

#### REFERENCES

- 1 Barot, N. R. and Elvidge, J. A. *J. Chem. Soc. Perkin I* 1972, 1009
- 2 Bailey, J. R. and Snyder, D. F. *J. Am. Chem. Soc.* 1915, **37**, 1915
- 3 Le Quesne, W. J. and Young, G. T. *J. Chem. Soc.* 1950, 1954
- 4 Gross, V. H. and Keitel, I. *J. Prakt. Chem.* 692, **311**, 1969
- 5 Schotten, C. *Ber.* 2544, **17**, 1884
- 6 Bauman, E. *Ber.* 3218, **19**, 1886

## Annealing of polyethylene crystals in the hexagonal phase

T. Asahi, Y. Miyamoto, H. Miyaji and K. Asai

Department of Physics, Faculty of Science, Kyoto University, Kyoto 606, Japan

(Received 28 September 1981)

The kinetics of thickening of polyethylene crystals in the hexagonal phase is studied. Distributions of thickness,  $L$ , of bands and/or lamellae are obtained by electron microscopy for a specimen annealed at  $p = 6.1$  kbar,  $T = 242^\circ C$  for 30, 300, 3600 and 86 400 seconds. The dependence of the average band thickness  $\bar{L}(t)$  on the annealing time  $t$  can be expressed as  $\bar{L}(t) = 46 \cdot \log(t/t_0) + \bar{L}(t_0)$  [nm]. Moreover, these distributions can be superposed on each other if we scale  $L$  by  $\bar{L}(t)$ . A model for the thickening process of a lamellae is proposed; coalescence of two bands occurs by disappearance of the boundary with the rate proportional to  $\exp(-\alpha L)$ . The value of  $\alpha$  depends on the mobility of defects in the boundary and is discussed in detail.

**Keywords** Polyethylene; high pressure; annealing; hexagonal phase; morphology; lamella

#### INTRODUCTION

Standard methods of crystallizing polyethylene, including melt- and solution-crystallization, give lamellar structures several tens of nm thick.

Wunderlich<sup>1</sup> first observed the band structure, several hundred nm thick (extended chain crystals, ECC), on crystallization under high pressure. Bassett<sup>2</sup> postulated that ECC are formed on crystallization under high pressure through the hexagonal phase. Several laboratories have attempted to verify this hypothesis and failed; the hexagonal phase was not always necessary for the formation of ECC<sup>3</sup>.

Effects of annealing on lamellar and/or band thickness have been reported<sup>4–6</sup>, and for a constant annealing time, lamellar thickness increases in the hexagonal phase much more rapidly than in the orthorhombic phase.

Here, the kinetics of lamellar thickening in the hexagonal phase are reported. A model of the thickening process involving coalescence of lamellae is proposed. The results of the simulation on this model are compared with the experimental results.

#### EXPERIMENTAL

The material used was unfractionated high density polyethylene, Sholex 6009 ( $M_n = 1.4 \times 10^4$ ,  $M_w = 1.14 \times 10^5$ ). The material was melt-crystallized at

atmospheric pressure, annealed at 120°C for 1 day, and then used. The long period obtained by small-angle X-ray scattering (SAXS) was 29 nm.

The high pressure differential thermal analysis (d.t.a.) cell used for annealing is shown in Figure 1. Pressure was measured by a calibrated manganine gauge using silicone oil as pressure transmitting fluid. Temperature was measured by a copper–constantan thermocouple.

A 7 mg sample for d.t.a. was pushed onto the thermocouple by a screw, and another sample for observation of fracture surface about  $12 \times 7 \times 1$  mm<sup>3</sup>, was placed into the slit shown in Figure 1. After elevating the pressure to ~6 kbar, the cell was heated at 5 K min<sup>-1</sup>. Samples were annealed for selected times at  $P = 6.1$  kbar and  $T = 242^\circ C$ , just above the temperature at which the orthorhombic → hexagonal phase occurs, as confirmed by d.t.a. Cooling to room temperature was then carried out at an initial rate of 60 K min<sup>-1</sup>. Annealing times were 30, 300, 3600 and 86 400 s.

Annealed samples were fractured in liquid nitrogen, and the fracture surfaces observed in an electron microscope using a two-stage replica technique. Crystal thickness distributions were obtained as follows. Two sets of parallel lines, mutually orthogonal, were drawn on the photographs at intervals of 440 nm. Crystal thickness was measured along the striation direction at the intersection

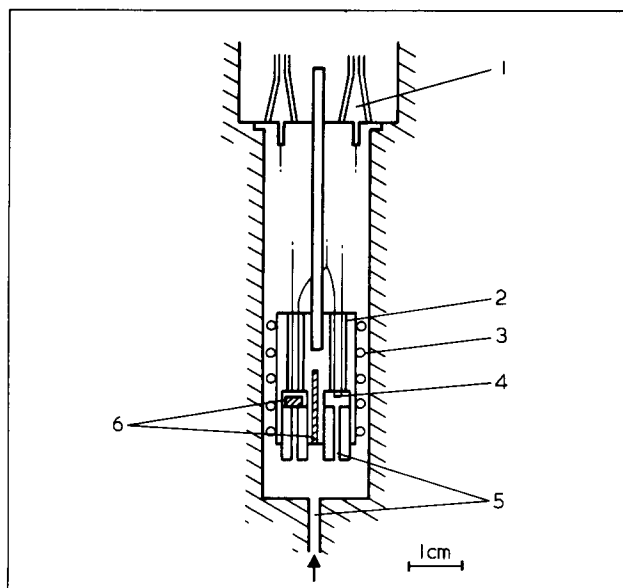


Figure 1 High pressure d.a. cell; (1) terminal; (2) alumina tube; (3) heater; (4) thermocouple; (5) inlet for oil; (6) samples

points and the data plotted as normalized histograms of frequency against crystal thickness at intervals of 21.3 nm. The total number of the measurements for each sample was 163–255.

RESULTS

Electron micrographs of replicated fracture surfaces of polyethylene after annealing are shown in Figure 2. The lamellae, or bands, are closely spaced, essentially occupying the entire surface area; the amorphous region is confined to the boundaries between the bands where these exist. As seen in Figure 2, the average band thickness increases with annealing time. Both average thickness and the width of the distribution increase with annealing time (Figure 3). It should be noted that the distribution of band lengths,  $L$ , obtained by the method described in the Experimental is a weight fraction  $W(L)$  given by the following equation:

$$W(L) = L \cdot N(L) / \int L \cdot N(L) dL \quad (1)$$

where  $N(L)$  is a number fraction.

Another interesting feature of these distributions is that each one can be superposed upon the other if we scale the abscissa by the average length  $\bar{L}$ ; the abscissa is thus  $L/\bar{L}$  instead of  $L$  (Figure 4). This implies that the ratio of the distribution width,  $\Delta L \equiv (\bar{L}^2 - \bar{L}^2)^{1/2}$ , to the average distribution,  $\bar{L}$ , is constant. Figure 5 shows the effects of annealing time on the average band thickness,  $\bar{L}$ , and distribution width;  $\bar{L}$  increases approximately linearly with the logarithm of annealing time,  $t$ ;

$$\bar{L}(t) = a \cdot \ln(t/t_0) + \bar{L}(t_0) \quad (2)$$

where  $a=46$  nm.  $\bar{L}$  and  $\Delta L$  are given for different annealing times in Table 1.

MODEL AND SIMULATION

The band thickening process for polyethylene has not yet been clarified. One possible mechanism is the formation of

a thickening nucleus on a lamella followed by the diffusion of chains to the nucleus<sup>7</sup>. This mechanism gives the same equation as equation (2). However, the mechanism implies narrowing of the lamellar thickness distribution function with annealing time. Moreover, the mechanism involves the formation of voids in thickened lamella. Therefore, we propose another mechanism for the thickening process in bulk specimens.

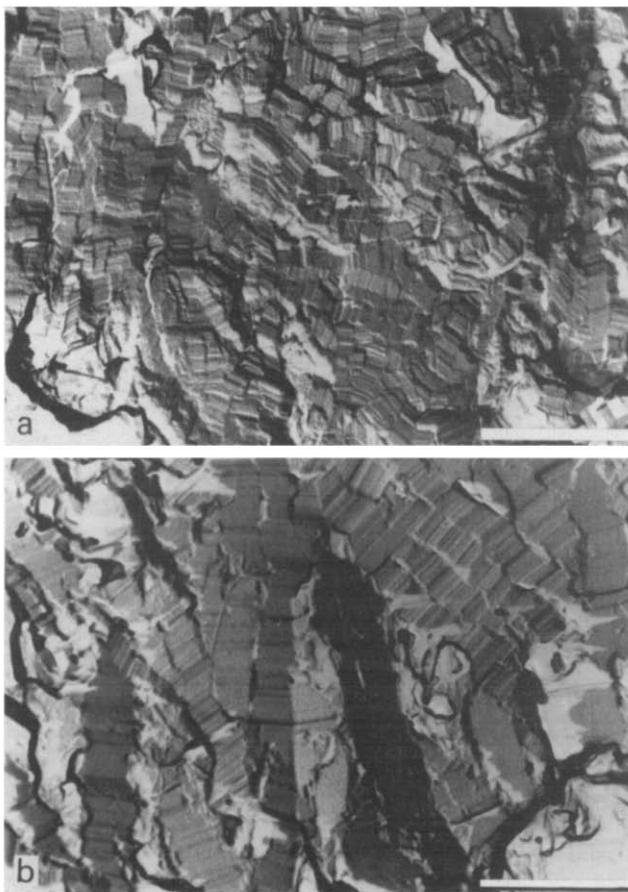


Figure 2 Electron micrographs of fracture surfaces of polyethylene after annealing in the hexagonal phase ( $P = 6.1$  kbar,  $T = 242^\circ\text{C}$ ) for the following times; (a), 30 s; (b) 86400 s. Scale bar, 1  $\mu\text{m}$

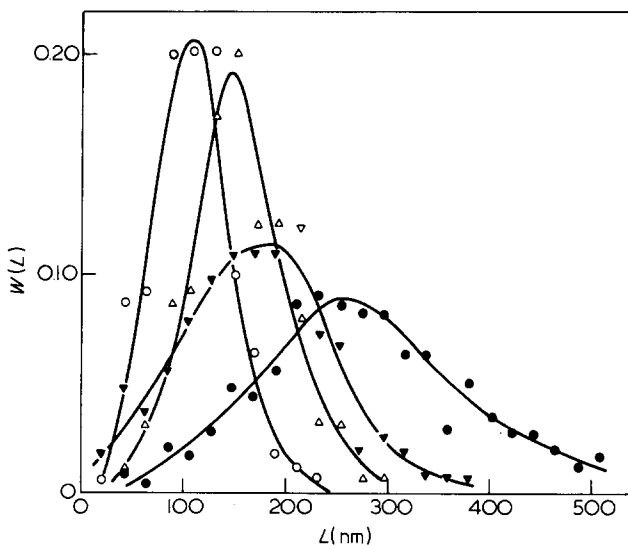


Figure 3 Distributions of band thickness of polyethylene crystals after annealing for:  $\circ$ , 30 s;  $\Delta$ , 300 s;  $\blacktriangle$ , 3600 s;  $\bullet$ , 86400 s.  $W(L)$  denotes weight fraction

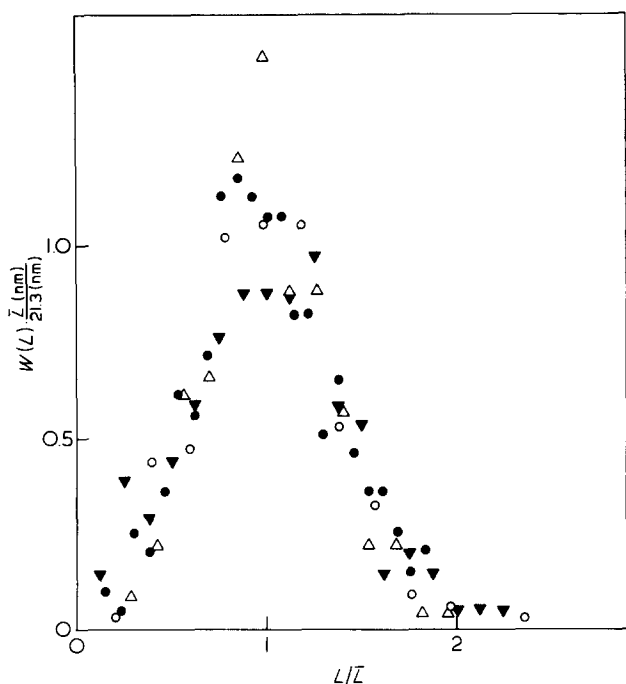


Figure 4 Normalized distributions of band thickness of polyethylene crystals after annealing for: ○, 30 s; △, 300 s; ▲, 3600 s; ●, 86400 s

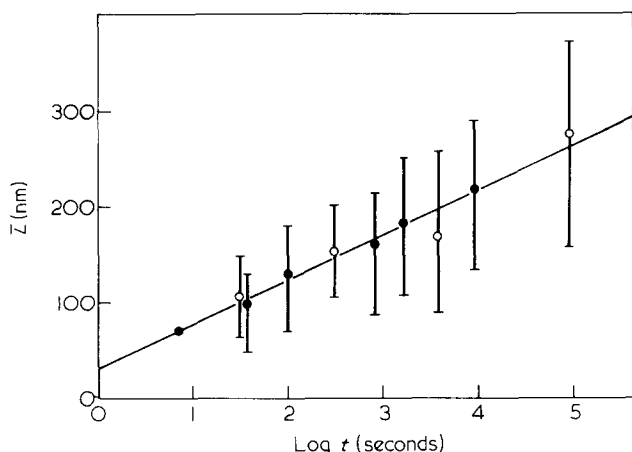


Figure 5 Time dependence of the average band thickness  $\bar{L}$ : ○, experiment; ●, simulation. Bars indicate the half-peak widths of the distributions. The points obtained by the simulation are displaced parallel to the abscissa in order to fit them to the experimental data

The original specimen has an average long period,  $\bar{L}_0$ , of 29 nm. This system is approximated by a one-dimensional perfect lattice, where the lattice points correspond to the boundaries between lamellae with a period of  $\bar{L}_0$ . Although we have some distribution around  $\bar{L}_0$ , we can neglect this distribution as far as bands thicker than 100 nm are concerned. Thickening is simulated by allowing lattice points to vanish randomly with time. If one lattice point vanishes, the distance between the neighbouring lattice points increases from  $\bar{L}_0$  to  $2\bar{L}_0$ . Clearly, this procedure gives an exponential function for the distribution of the distance  $L$  between the neighbouring lattice points. For the weight fraction  $W_R(L)$ , we get the following equation, using a parameter  $\alpha$ :

$$W_R(L) = \alpha^2 L \exp(-\alpha L)$$

$$\bar{L} = 2/\alpha, \quad \Delta L = (\bar{L}^2 - \bar{L}^2)^{1/2} = \sqrt{2}/\alpha \quad (3)$$

This distribution gives a constant ratio  $(1/\sqrt{2})$  of  $\Delta L$  to  $\bar{L}$  and agrees with one of the experimental results. However, the value of  $L_p$  for which  $W_R(L)$  is a maximum is given by  $\bar{L}/2$ . The value is too small when compared with the experimental result,  $L_p \approx \bar{L}$ .

To improve this, we weight the probability for vanishing of lattice points. It is reasonable to assume that a lattice point separated by a large distance from its nearest neighbour takes a longer time to vanish than one separated by a short distance. A lattice point at a distance of  $n\bar{L}_0$  from the closer of its two neighbours is assumed to take a time proportional to  $m^n$  to vanish ( $m = \text{constant}$ ). This will be discussed below.

A system containing  $10^4$  numbered lattice points has been simulated. Random numbers from 1 to 10 000 were produced successively. When a random number coincides with a lattice point, that lattice point vanishes only when the shorter of the two nearest neighbour distances is  $n\bar{L}_0$  and there are  $m^{n-1}$  times of coincidence.

The advantage of this simulation is that the time elapsed corresponds to the times to produce the random numbers. Thus the kinetics of the thickening process are automatically taken into account.

The results of the simulation for the  $10^4$  lattice points are shown in Figure 6. The thickness distribution,  $L$ , agrees fairly well with the experimental value; the ratio of average thickness  $\bar{L}$  to  $\Delta L$  is constant ( $\sim 1.2$ ) and the ratio of  $\bar{L}$  to  $L_p$  is about 1. Figure 5 shows the time dependence of the average band thickness  $\bar{L}$  upon  $\Delta L$ . Best fit to the experimental data gives  $m = 10$ .

Table 1 Average band thickness,  $\bar{L}$ , and the width of the distribution for annealing time  $t$

$t$ (s)	$\bar{L}$ (nm)	$\Delta L$ (nm)
30	107	39
300	151	48
3600	169	72
86 400	275	99

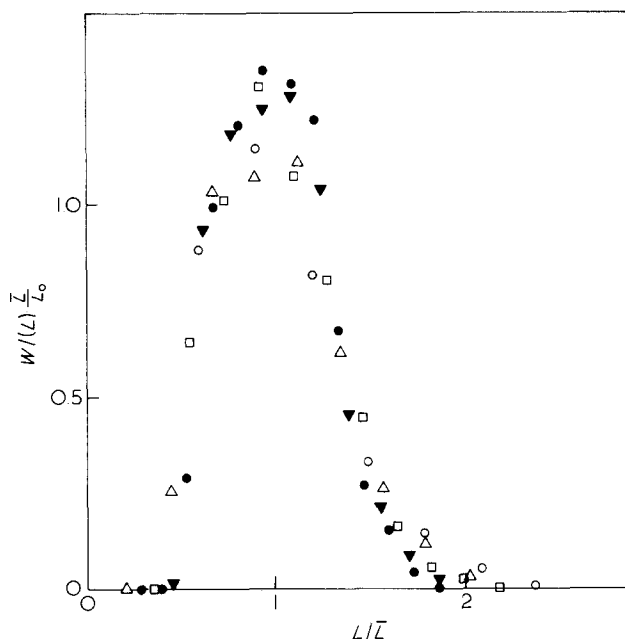


Figure 6 Normalized distributions of band thickness obtained by the simulation with  $m = 10$ : ○,  $\bar{L} = 3.37 \bar{L}_0$  and  $S = 43\,528$ ; △,  $\bar{L} = 4.47 \bar{L}_0$  and  $S = 115\,141$ ; □,  $\bar{L} = 5.50 \bar{L}_0$  and  $S = 967\,824$ ; ▲,  $\bar{L} = 6.46 \bar{L}_0$  and  $S = 1\,887\,050$ ; ●,  $\bar{L} = 7.51 \bar{L}_0$  and  $S = 10\,379\,283$ .  $S$  denotes the times to produce the random numbers

## DISCUSSION

In modelling band thickening, boundaries between bands are allowed to disappear with time. A physical representation of this model is the coalescence of two bands. We treat the boundaries as planes including many defects rather than as an amorphous region. The hexagonal phase contains many chain defects<sup>8</sup>. Therefore when a crystal transforms orthorhombic to hexagonal phase, the boundary defects can easily migrate through the crystals along the chain axis. Eventually the defect will be excluded from the crystal to the surface, i.e. another boundary; thus the two bands coalesce. Although the diffusion along the chain is fast in the hexagonal phase, a defect can be trapped in the lamella. With a mean path between trapping sites,  $\lambda$ , and trapping energy,  $E$ , the rate at which defects vanish,  $R_D$ , is as follows:

$$R_D \propto \exp(-LE/\lambda kT) \quad (4)$$

where  $k$  is the Boltzmann constant and  $T$  is the absolute temperature. The thickening rate of the band,  $d\bar{L}/dt$ , is then given by:

$$d\bar{L}/dt = R_D \bar{L} \propto [\exp(-LE/\lambda kT)] \bar{L} \quad (5)$$

A neighbour vanishes when a distance between boundaries,  $\bar{L}$ , exists, and thus the contribution to the thickening rate  $d\bar{L}/dt$  is approximately proportional to  $\bar{L}$ .

It is easily shown that equation (5) is essentially a straight line for the curve  $\bar{L}$  against  $\log t$ . The essential point in equation (4) is that a factor proportional to  $L$  is included in the exponent; this is the reason why the probability for vanishing of a defect is weighted by  $m^{-n}$  in the simulation:  $L = n\bar{L}_0$ . Comparing  $m$  obtained from the simulation with the experimental curve, we obtain  $2.3kT$  for the value of  $(E/\lambda)\bar{L}_0$ . For  $T \approx 500\text{K}$ ,  $(E/\lambda)\bar{L}_0$  is about  $2.3 \text{ kcal mol}^{-1}$ . This value is not surprising though its validity is open to discussion. For annealing in the orthorhombic phase, the value of  $E/\lambda$  is much larger, presumably due to both smaller  $\lambda$  and larger  $E$ .

Thus it has been shown that band structure can be formed by annealing through the coalescence of lamellae. Even annealing in the orthorhombic phase for a long period would give the band structure.

## REFERENCES

- 1 Wunderlich, B. and Arakawa, T. *J. Polym. Sci. (A)* 1964, **2**, 3697
- 2 Bassett, D. C. and Turner, B. *Phil. Mag.* 1974, **29**, 925
- 3 Yasuniwa, M., Nakafuku, C. and Takemura, T. *Polym. J.* 1973, **4**, 526
- 4 Gruner, C. L., Wunderlich, B. and Bopp, R. C. *J. Polym. Sci. (A-2)* 1969, **7**, 2099
- 5 Bassett, D. C. and Carder, D. R. *Phil. Mag.* 1973, **28**, 513
- 6 Bassett, D. C., Khalifa, B. A. and Olley, R. H. *Polymer* 1976, **17**, 284
- 7 Hirai, N., Mitsuhashi, T. and Yamashita, Y. *Rep. Res. Lab. Surface Sci. Fac. Sci. Okayama Univ.* 1961, **2**, 1
- 8 Yamamoto, T. *J. Macromol. Sci. (B)* 1979, **16**, 487

## Stability of the crystal structures of poly(vinyl alcohol) (PVA) by CNDO/2 calculations

Masaru Ohsaku, Toshie Hatamoto, and Hiromu Murata

Department of Chemistry, Faculty of Science, Hiroshima University, Higashisenda-machi, Hiroshima 730, Japan

and Akira Imamura

Department of Chemistry, Shiga University of Medical Science, Setatsukinowa-cho, Otsu, Shiga 520-21, Japan

(Received 4 November 1980)

CNDO/2 calculations using the tight-binding approximation for polymers was applied to poly(vinyl alcohol) (PVA). The calculations were performed assuming several crystal structures. The stability among the structures was explained by using the calculated results in connection with the hydrogen bonding involved.

**Keywords** Stability; crystal structure; poly(vinyl alcohol), CNDO/2 calculations; semi-empirical MO; MO procedure; hydrogen bonding

We have previously presented<sup>1</sup> the results of the CNDO/2 calculations<sup>2</sup> on poly(hydroxymethylene) (PHM) and poly(vinyl alcohol) (PVA) using these molecules as models of the poly(saccharide).

The relative conformational stability among four forms of PHM and between two forms of PVA can be reasonably explained by these calculations, and we have obtained information about the stability of the ring part of the saccharides.

However, we were unable to obtain information on the crystal structure of PVA, because we were considering only a single polymer chain.

Several models for the PVA crystal have been proposed and investigated<sup>3-7</sup>. Among these, Bunn's<sup>3a</sup> and

Sakurada's<sup>3b</sup> models are well documented.

Here, we investigate which model is most suitable in describing the crystal structure of PVA, using CNDO/2 methods in conjunction with the tight-binding approximation<sup>8</sup>.

We designate Bunn's model as Model I and Sakurada's model as Model II. Calculations were carried out on an isotactic form of PVA. Numerical calculations were performed as in the previous papers<sup>9,10</sup>. Geometries used for the calculations are listed in Table I. Distance  $a$  (Figure 1) was allowed to take values 2.8, 3.0, and 3.2 Å.

Two structures were studied for each model: in the first, the group O-H...O was assumed to be straight; in the other the angle  $\phi(\text{COH})$  was taken to be  $105.937^\circ$ <sup>11</sup>. The